

On the Black Hole Mass - Bulge Mass Relation

Nadine Häring and Hans-Walter Rix

Max-Planck Institute for Astronomy, Heidelberg

`haering@mpia-hd.mpg.de` and `rix@mpia-hd.mpg.de`

ABSTRACT

We have re-examined the relation between the mass of the central black holes in nearby galaxies, M_{bh} , and the stellar mass of the surrounding spheroid or bulge, M_{bulge} . For a total of 30 galaxies bulge masses were derived through Jeans equation modeling or adopted from dynamical models in the literature. In stellar mass-to-light ratios the spheroids and bulges span a range of a factor of eight. The bulge masses were related to well-determined black hole masses taken from the literature. With these improved values for M_{bh} , compared to Magorrian et al. (1998), and our redetermination of M_{bulge} , we find the $M_{bh} - M_{bulge}$ relation becomes very tight. We find $M_{bh} \sim M_{bulge}^{1.12 \pm 0.06}$ with an observed scatter of $\lesssim 0.30$ dex, a fraction of which can be attributed to measurement errors. The scatter in this relation is therefore comparable to the scatter in the relations of M_{bh} with σ and the stellar concentration. These results confirm and refine the work of Marconi and Hunt (2003). For $M_{bulge} \sim 5 \times 10^{10} M_\odot$ the median black hole mass is $0.14\% \pm 0.04\%$ of the bulge mass.

Subject headings: galaxies: bulges — galaxies: kinematics and dynamics

1. Introduction

The good correlations between the mass of the central black hole and the physical properties of the surrounding stellar bulge provides evidence that black holes play a key role in the evolution of galaxies. So far, the tightest relation is that between the black hole mass M_{bh} and the stellar velocity dispersion σ of the bulge stars (Ferrarese and Merritt 2000; Gebhardt et al. 2000a). Apart from that, other properties correlate with the mass of the black hole at the center of galaxies. Graham et al. (2002) showed that M_{bh} correlates tightly with the concentration of the host bulge as quantified by the Sersic index n . Magorrian et al. (1998) explored the relation between M_{bh} and bulge mass, M_{bulge} , finding $M_{bh} \sim 0.005 M_{bulge}$, but with very large scatter. It is timely to reconsider this relation, since black hole mass measurements, now mostly based on HST data, have become much more reliable. In fact it is now clear that the black hole masses modeled by Magorrian et al. (1998) were overestimated by as much as a factor of ten, since the black hole's sphere of gravitational influence was not well resolved in their data. This necessarily implies that the black

hole mass fraction is lower than originally estimated (Merritt and Ferrarese 2001).

Recently, Marconi and Hunt (2003) showed that in the near infrared the correlation of the bulge luminosity and the black hole mass becomes much tighter than in the optical. They also demonstrated a tight relation between $R_e\sigma_e^2$ and the black hole masses, where $R_e\sigma_e^2$ represents a simple virial bulge mass estimate.

In this Letter we explore further the connection between the mass of the central black hole and the dynamical mass of the galaxy’s bulge or spheroid in more detail, by combining direct M_{bh} estimates, deemed reliable from other work, with M_{bulge} determinations based on Jeans equation modeling, as opposed to virial estimates.

2. The sample

Our sample consists of 30 nearby galaxies, mostly early types, with existing reliable black hole mass estimates, of which 27 were drawn from Tremaine et al. (2002). In addition, the black hole mass for NGC4594 is taken from Kormendy (1988), for NGC7332 from Gebhardt (private communication), and for NGC4374 from Maciejewski and Binney (2001). For the Milky Way the black hole mass is from Schödel et al. (2002). For convenience the appropriate references are listed in Table 1. The selection criteria were first the reliability of the black hole mass and second the availability of either modeled bulge masses or of surface-brightness and velocity dispersion profiles, needed for the dynamical modeling of the bulge masses.

For 12 of the galaxies we adopted the bulge masses from Magorrian et al. (1998), derived by them through Jeans equation modeling, after checking that our modeling (cf. §3) were consistent for these objects. In addition, we took the bulge masses for NGC1023 from Bower et al. (2001), for NGC3245 from Barth et al. (2001), for NGC4342 from Cretton and van den Bosch (1999) and for NGC3384, for NGC4697, for NGC5845 and for NGC7457 from Gebhardt et al. (2003).

The Milky Way is a special case, since the black hole mass is by far the most secure but the uncertainty in the bulge mass (mostly conceptual) is yet quite high. Different groups state different values for the bulge mass. The value $1.1 \times 10^{10} M_\odot$ is taken from Bissantz et al. (1997) and is in agreement with Dwek et al. (1995).

Our sample selection should not introduce any significant bias towards a particular relation between M_{bh} and M_{bulge} or affect the scatter in such a relation. The galaxy properties are summarized in Table 1, where group 1 denotes the galaxies modeled as part of this work, and the bulge masses for group 2 galaxies were adopted from the literature. The distances are taken from Tonry et al. (2001) for most of the galaxies; where these are not available, the distance is determined from the recession velocity, assuming a Hubble constant of $70 \text{ km s}^{-1} \text{ Mpc}^{-1}$.

3. The dynamical modeling

To model the bulge masses of the galaxies in the sample we chose the most straightforward approach that improves on M_{bulge} estimates from luminosities or from virial estimates, yet reflects in its simplicity the inhomogeneous and often scarce kinematic data at larger radii. Specifically, we solved the Jeans equation in its spherical form:

$$\frac{d(\rho_\star \sigma_r^2)}{dr} + 2 \frac{\beta \rho_\star \sigma_r^2}{r} = -\rho_\star \frac{d\Phi_\star}{dr}, \quad (1)$$

where r is the radius, ρ_\star is the stellar mass density of the bulge, σ_r is the stellar radial velocity dispersion, β measures the anisotropy in the velocity, and Φ_\star is the total potential due to the stars. In the radial range we cover ($1'' \lesssim r \lesssim 30''$), we neglect any explicit contribution from the dark matter halo. This modeling procedure is similar to the technique described by van der Marel (1994). We assumed the galaxies to be isotropic ($\beta = 0$) and spherically symmetric, which might lead to an overestimation of the mass. But as Kochanek (1994) showed, this leads to a peak error of not more than 5% for the velocities. We verified this approach by comparison with the axisymmetric models of Magorrian et al. (1998). As boundary conditions for the modeling we set both the velocity and its first derivative to vanish at the outer edge of the bulge, which we assume to have a finite mass. Since the boundary conditions are set at the outer border of the system, solving Jeans' equation from the outside to the inside is the appropriate choice.

The procedure is as follows:

- 1) We fit a surface brightness model to the published photometry, modeling the luminosity density as a broken power law, where the inner and outer slopes can be fit independently:

$$j(r) = j_0 (r/a)^{-\alpha} \left(1 + (r/a)^2\right)^{-\beta}, \quad (2)$$

with r taken along the major axis of the bulge. The typical radial range for the fitted profiles extends from $1''$ to $25''$. For these large apertures a seeing correction is not necessary. All systems, except NGC1068, are bulge dominated and a bulge-to-disk decomposition is not critical. For NGC1068 we perform a one dimensional bulge-to-disk decomposition to only account for the bulge stars.

- 2) A constant mass-to-light ratio Υ is assumed to convert the luminosity density into the mass density and calculate the potential.
- 3) The Jeans equation in its spherical and isotropic form is solved using a fourth order Runge-Kutta algorithm, predicting the velocity dispersion $\sigma_r(r)$ for each galaxy.
- 4) The dispersions are integrated along the line-of-sight, projected back onto the plane of the sky, averaged over the observational aperture and compared to the kinematic data. The observed velocity profiles typically extend from $2''$ to $25''$. For these apertures seeing convolution is neglected.
- 5) From this the value for Υ is adjusted by scaling the model velocity dispersion curve to best match the observed values. The mass of the central black hole is unchanged during the scaling procedure. Two examples of this modeling procedure are shown in Figure 1.
- 6) Using this final value for Υ , the mass density is integrated over the galaxy's bulge (with

Table 1: Summary of galaxy properties

Galaxy (1)	Type (2)	$M_{\text{bh}} [\text{M}_{\odot}]$ (3)	Ref (4)	$\sigma [\text{km/s}]$ (5)	$L_{\text{bulge}} [\text{L}_{\odot}]$ (6)	$\Upsilon, \text{Band} [\text{M}_{\odot}/\text{L}_{\odot}]$ (7)	$M_{\text{bulge}} [\text{M}_{\odot}]$ (8)	Ref (9)	dist [Mpc] (10)
group 1									
M87	E0	$3.0^{+1.0}_{-1.0} \cdot 10^9$	1	375	$2.0 \cdot 10^{11}$	3.0,I	$6.0 \cdot 10^{11}$	22, 23, 24	16.1
NGC1068	Sb	$1.4^{+1.3}_{-0.7} \cdot 10^7$	2	151	$1.5 \cdot 10^{11}$	0.15,R	$2.3 \cdot 10^{10}$	25, 26, 27	15.0
NGC3379	E1	$1.0^{+0.6}_{-0.5} \cdot 10^8$	3	206	$1.7 \cdot 10^{10}$	4.0,R	$6.8 \cdot 10^{10}$	28, 29	10.6
NGC4374	E1	$4.3^{+3.2}_{-1.7} \cdot 10^8$	4	296	$6.0 \cdot 10^{10}$	6.0,R	$3.6 \cdot 10^{11}$	30, 23, 24	18.4
NGC4261	E2	$5.2^{+1.0}_{-0.5} \cdot 10^8$	5	315	$4.5 \cdot 10^{10}$	8.0,R	$3.6 \cdot 10^{11}$	30, 23, 24	31.6
NGC6251	E2	$5.3^{+2.0}_{-1.0} \cdot 10^8$	6	290	$9.3 \cdot 10^{10}$	6.0,R	$5.6 \cdot 10^{11}$	31, 32	106.0
NGC7052	E4	$3.3^{+2.3}_{-1.3} \cdot 10^8$	7	266	$8.3 \cdot 10^{10}$	3.5,R	$2.9 \cdot 10^{11}$	33, 28, 34	58.7
NGC4742	E4	$1.4^{+0.4}_{-0.5} \cdot 10^7$	8	90	$6.2 \cdot 10^9$	1.0,R	$6.2 \cdot 10^9$	28, 35	15.5
NGC821	E4	$3.7^{+1.7}_{-1.5} \cdot 10^7$	9	209	$2.9 \cdot 10^{10}$	4.5,R	$1.3 \cdot 10^{11}$	28, 29	24.1
IC1459	E3	$2.5^{+0.5}_{-0.4} \cdot 10^9$	10	323	$6.9 \cdot 10^{10}$	4.2,R	$2.9 \cdot 10^{11}$	36, 37	29.2
group 2									
M31	Sb	$4.5^{+4.0}_{-2.5} \cdot 10^7$	11	160	$7.3 \cdot 10^9$	5.1,V	$3.7 \cdot 10^{10}$	12	0.76
M32	E2	$2.5^{+0.5}_{-0.5} \cdot 10^6$	13	75	$3.8 \cdot 10^8$	2.1,V	$8.0 \cdot 10^8$	12	0.81
NGC1023	SB0	$4.4^{+0.5}_{-0.5} \cdot 10^7$	14	205	$1.2 \cdot 10^{10}$	5.8,V	$6.9 \cdot 10^{10}$	14	11.4
NGC2778	E2	$1.4^{+1.6}_{-0.8} \cdot 10^7$	9	175	$1.2 \cdot 10^{10}$	6.6,V	$7.6 \cdot 10^{10}$	12	22.9
NGC3115	S0	$1.0^{+1.0}_{-0.6} \cdot 10^9$	15	230	$1.7 \cdot 10^{10}$	7.0,V	$1.2 \cdot 10^{11}$	12	9.7
NGC3245	S0	$2.1^{+1.0}_{-0.6} \cdot 10^8$	16	205	$1.7 \cdot 10^{10}$	3.7,R	$6.8 \cdot 10^{10}$	16	20.9
NGC3377	E5	$1.0^{+0.9}_{-0.2} \cdot 10^8$	9	145	$6.4 \cdot 10^9$	2.5,V	$1.6 \cdot 10^{10}$	12	11.2
NGC3384	S0	$1.6^{+0.2}_{-0.1} \cdot 10^7$	9	143	$7.1 \cdot 10^9$	2.8,V	$2.0 \cdot 10^{10}$	9	11.6
NGC3608	E2	$1.9^{+1.0}_{-0.6} \cdot 10^8$	9	182	$1.9 \cdot 10^{10}$	5.2,V	$9.7 \cdot 10^{10}$	12	23.0
NGC4291	E2	$3.1^{+1.3}_{-1.1} \cdot 10^8$	9	242	$1.9 \cdot 10^{10}$	6.9,V	$1.3 \cdot 10^{11}$	12	26.2
NGC4342	S0	$3.0^{+1.7}_{-1.0} \cdot 10^8$	17	225	$1.9 \cdot 10^9$	6.3,I	$1.2 \cdot 10^{10}$	17	15.3
NGC4473	E5	$1.1^{+0.4}_{-0.3} \cdot 10^8$	9	190	$1.8 \cdot 10^{10}$	5.2,V	$9.2 \cdot 10^{10}$	12	15.7
NGC4564	E3	$5.6^{+0.3}_{-0.7} \cdot 10^7$	9	162	$8.1 \cdot 10^9$	5.4,V	$4.4 \cdot 10^{10}$	12	15.0
NGC4594	Sa	$1.0^{+1.0}_{-0.7} \cdot 10^9$	18	240	$4.4 \cdot 10^{10}$	6.1,V	$2.7 \cdot 10^{11}$	12	9.8
NGC4649	E1	$2.0^{+0.5}_{-1.0} \cdot 10^9$	9	375	$6.1 \cdot 10^{10}$	7.9,V	$4.9 \cdot 10^{11}$	12	16.8
NGC4697	E4	$1.7^{+0.2}_{-0.1} \cdot 10^8$	9	177	$2.3 \cdot 10^{10}$	4.7,V	$1.1 \cdot 10^{11}$	9	11.7
NGC5845	E3	$2.4^{+1.4}_{-1.4} \cdot 10^8$	9	234	$6.7 \cdot 10^9$	5.5,V	$3.7 \cdot 10^{10}$	9	25.9
NGC7332	S0	$1.3^{+0.6}_{-0.5} \cdot 10^7$	19	122	$7.9 \cdot 10^9$	1.9,V	$1.5 \cdot 10^{10}$	12	23.0
NGC7457	S0	$3.5^{+1.1}_{-1.4} \cdot 10^6$	9	67	$2.1 \cdot 10^9$	3.4,V	$7.0 \cdot 10^9$	9	13.2
Milky Way	SBbc	$3.7^{+1.5}_{-1.5} \cdot 10^6$	20	75			$1.1 \cdot 10^{10}$	21	

NOTES. - (1) Galaxy name. (2) Morphological type from de Vaucouleurs et al. (1991). (3) Black hole mass taken from Tremaine et al. (2002). (4) References for the black hole masses. (5) Stellar velocity dispersions from Tremaine et al. (2002). (6) Bulge luminosity modeled as part of this work (group 1) and adapted from the literature (group 2). (7) Mass-to-light ratio derived from the Jeans modeling (group 1) and adapted from the literature. (8) Modeled bulge mass (group 1) and adapted form the literature (group 2). (9) References for the photometric and kinematic data used for the modeling (group 1) and for the adopted bulge masses (group 2). (10) Galaxy distance.

REFERENCES. - (1) Ford et al. 1994, (2) Greenhill and Gwinn 1997, (3) Gebhardt et al. 2000b, (4) Maciejewski and Binney 2001, (5) Ferrarese et al. 1996, (6) Ferrarese and Ford 1999, (7) van der Marel and van den Bosch 1998, (8) Tremaine et al. 2002, (9) Gebhardt et al. 2003, (10) Cappellari et al. 2002, (11) Tremaine (1995), (12) Magorrian et al. 1998, (13) Verolme et al. 2002, (14) Bower et al. 2001, (15) Kormendy et al. 1996, (16) Barth et al. 2001, (17) Cretton and van den Bosch 1999, (18) Kormendy 1988, (19) Gebhardt (priv. comm.), (20) Schödel et al. 2002, (21) Bissantz et al. 1997

PHOTOMETRIC AND SPECTROSCOPIC DATA USED FOR THE MODELING (22) Lauer et al. 1992, (23) Peletier et al. 1990, (24) Davies and Birkinshaw 1988, (25) Sánchez-Portal et al. 2000, (26) Peletier et al. 1999, (27) Dressler 1984, (28) Lauer 1985, (29) Bender et al. 1994, (30) Ferrarese et al. 1994, (31) Ferrarese and Ford 1999, (32) Heckman et al. 1985, (33) van den Bosch and van der Marel 1995, (34) Di Nella et al. 1995, (35) Davies et al. 1983, (36) Franx et al. 1989, (37) Fried and Illingworth 1994

$r_{max} = 3r_{eff}$, where the mass of the bulge has already converged).

7) To account for the flattening of the bulge the bulge mass is multiplied by $\sqrt{1 - \epsilon}$, where ϵ is the projected ellipticity (e.g. Kochanek 1994).

The resulting bulge masses determined in this paper are listed in Table 1 (group1), augmented by bulge masses taken from the literature (group2). We re-modeled three bulge masses from the sample of Magorrian et al. (1998) and found good agreement:

$M_{M98}/M_{here}(M87) = 1.3$, $M_{M98}/M_{here}(NGC821) = 1.0$, and $M_{M98}/M_{here}(NGC3379) = 1.03$.

Also in other objects, the mass to light ratio from our spherical Jeans models agree well with the ones from much more extensive modeling: for IC1459 Cappellari et al. (2002) give $\Upsilon_I = 3.2$. At a mean color of $(R-I) \sim 1/2$ ($V-I \sim 0.65$) this corresponds to $\Upsilon_R = 4.1$, well in agreement with our value, $\Upsilon_R = 4.2$. For M87 van der Marel (1994) found $\Upsilon_I = 2.9$ in good agreement with our value, $\Upsilon_I = 3.0$. This comparison with a number of other authors show that our models, though more simplistic than other current approaches, provide sufficiently robust and unbiased estimates of M_{bulge} .

To account for the uncertainties introduced by the simplifying assumptions in the modeling (eg. spherical symmetry, isotropy, constant mass-to-light ratio) and the inhomogeneity of the data, we give a conservative individual error estimate for the bulge masses of a factor of 1.5 or $\pm 0.18\text{dex}$.

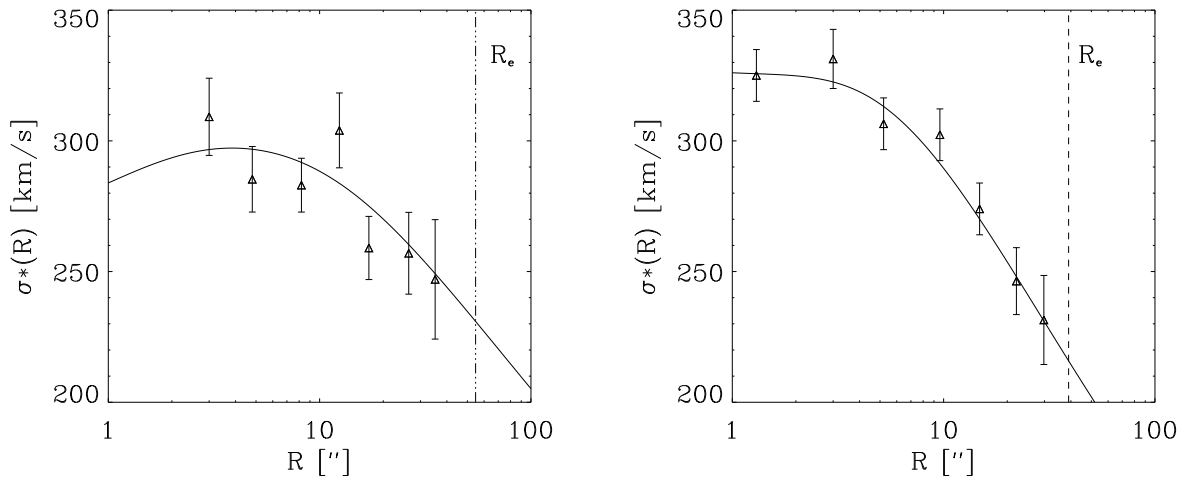


Fig. 1.— Two typical examples for the modeling are shown. The solid line gives the modeled velocity profile for NGC4374 (left panel) and NGC4261 (right panel). The quantity σ^* denotes the rms velocity of the stars ($\sqrt{\sigma^2 + v^2}$). Over-plotted are the data points observed by Davies and Birkinshaw (1988). The effective radius, R_e , is indicated by the dashed line. The modeled velocity profiles match the data well within the observed error bars.

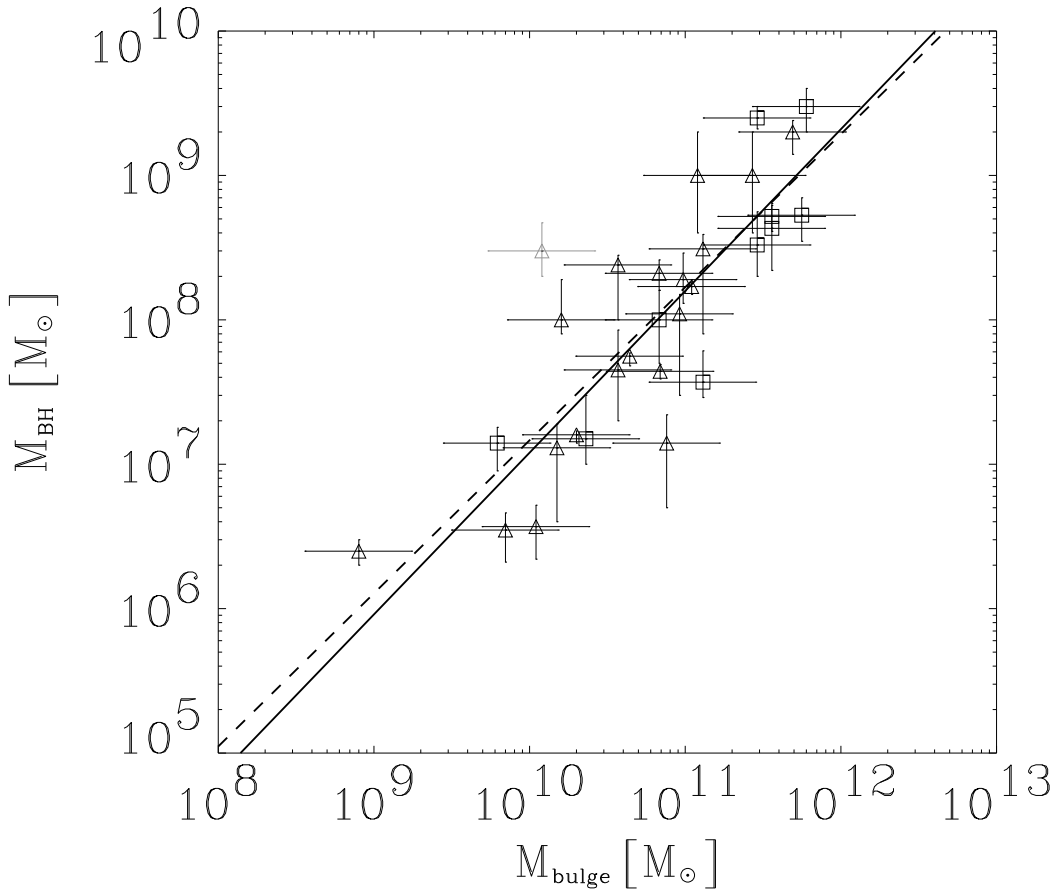


Fig. 2.— Black hole mass vs. bulge mass for the 30 sample galaxies. The solid line gives the bisector linear regression fit (see §4) to the data with a slope of 1.12 ± 0.06 . For comparison the relation found by Marconi and Hunt (2003) is shown as the dashed line (slope: 1.06 ± 0.09). The squares indicate galaxies taken from group 1 in Table 1 the triangles refer to group 2 galaxies. The error bars in black hole mass are the published ones given in Table 1 and for the bulge mass were adopted to be 0.18 dex in $\log(M)$ for all objects. The possible outlier, plotted in light grey is NGC4342 which was not included in the fit.

4. Results and Discussion

In Figure 2, we plot M_{bh} against the dynamical bulge mass M_{bulge} for the 30 galaxies in the sample. In contrast to the relation presented by Magorrian et al. (1998), there is a tight relation without strong outliers.

A bisector linear regression fit (Akritas and Bershady 1996) to the data leads to the relation

$$\log(M_{bh}/M_\odot) = (8.20 \pm 0.10) + (1.12 \pm 0.06) \log(M_{bulge}/10^{11} M_\odot),$$

where we included constant fractional errors of 0.18 dex on the bulge mass, the published uncertainties for the black hole masses (see Table 1), and an intrinsic scatter of 0.3 dex. For this fit we have excluded the one possible outlier, NGC 4342; its inclusion leaves the slope of the relation unchanged. We calculated the mean values and their 1σ uncertainties using the bootstrap method (Efron and Tibshirani 1993). Bootstrapping is preferable, since we do not have rigorous error bars for M_{bulge} , or for all M_{bh} estimates. Whether we adopt intrinsic scatter or δM_{bulge} of 0.2 dex or 0.3 dex for the fit changes the slope by $\lesssim 1\%$ and the intercept by less than 0.3%. A least squares fit using the FITEXY routine (Press et al. 1992) changes the slope by $\sim 15\%$, yielding 1.32 ± 0.17 . All values agree within the stated uncertainties.

The upper limit on the intrinsic dispersion in the $M_{bh} - M_{bulge}$ relation, namely the observed dispersion assuming no measurement errors, is ~ 0.30 dex. A significant portion of this scatter can plausibly be attributed to the observational errors in black hole masses. The implied median black hole mass fraction at bulge masses of $\sim 5 \times 10^{10} M_\odot$ is $M_{bh}/M_{bulge} = (1.4 \pm 0.4) \cdot 10^{-3}$. This fraction is in agreement with the estimates from Merritt and Ferrarese (2001) and Marconi and Hunt (2003).

At face value, the slope of the $M_{bh} - M_{bulge}$ relation exceeds unity with 1.5σ significance, both for the Akritas & Bershady estimator and the FITEXY routine, as also used by Marconi and Hunt (2003). However, the data are still in agreement with a $M_{bh} - M_{bulge}$ proportionality at the $< 2\sigma$ level and we do not want to emphasize the non-linearity.

The mass-to-light ratios Υ we found through the dynamical models are spread over a wide range from 0.15 to $8.0 M_\odot/L_\odot$. Excluding the smallest value, which comes from NGC1068 (a galaxy with starburst activity), we still find a range for Υ of a factor of eight.

Revisiting the Magorrian relation with more reliable black hole masses leads to a relation with a strongly reduced scatter. Our relation shows at most one outlier (NGC4342, among 30 objects) and we did not apply any selection criteria apart from the reliability of the black hole masses.

Our results confirm and expand the findings of Marconi and Hunt (2003), who relate black hole masses to infrared luminosities and also to virial bulge mass estimates ($M \sim \sigma^2 r_e$). Their $M_{bh} - M_{bulge}$ relation for all galaxies is statistically in agreement with the relation we find. They find a slightly higher observed scatter, potentially because their virial estimate is less precise than

the Jeans equation estimates, used here.

Through determining and compiling M_{bulge} measurements for the objects with robust M_{bh} estimates, we could demonstrate that the scatter in the black hole mass to bulge mass relation is nearly as small as that in the $M_{bh} - \sigma$ (Gebhardt et al. 2000a; Ferrarese and Merritt 2000) (~ 0.3 dex) and M_{bh} -concentration (Graham et al. 2002) (~ 0.31 dex) relation. Therefore, the relation between the black hole mass and the velocity dispersion is not unique and it seems as if the large scatter in the original Magorrian relation is due to erroneous estimation of the black hole masses.

Still, in the local universe $M - \sigma$ is of invaluable practical use, since velocity dispersions are easy to measure. However, towards higher redshift ($z \gtrsim 2$) the relation between black hole mass and stellar bulge mass gains importance. It is then exceedingly difficult to measure the velocity dispersion, but the bulge mass can be estimated via the measured luminosity and an upper limit of the stellar mass-to-light ratio, derived from the maximal age of the stellar population at that redshift.

We thank Andi Burkert for stimulating discussions on this paper, and Tim de Zeeuw and Michele Cappellari for useful comments. We thank the anonymous referee for a thorough and constructive report that helped to improve the manuscript.

REFERENCES

- Akritas, M. G. and Bershady, M. A. 1996, ApJ, 470, 706
- Barth, A. J., Sarzi, M., Rix, H. W., Ho, L. C., Filippenko, A. V. and Sargent, W. L. 2001, ApJ, 555, 685
- Bender, R., Saglia, R. P., Gerhard, O. E. 1994, MNRAS, 269, 785
- Bissantz, N., Englmaier, P., Binney, J. and Gerhard, O. 1997, MNRAS, 289, 651
- Bower, G. A. et al. 2001, ApJ, 550, 75
- Cappellari, M., Verolme, E. K., van der Marel, R. P., Verdoes Kleijn, G.A., Illingworth, G. D., Franx, M., Carollo, C. M., de Zeeuw, P. T. 2002 ApJ, 578, 787
- Cretton, N. & van den Bosch, F. 1999, ApJ, 514, 704
- Davies, R. L., Efstathiou, G., Fall, S. M., Illingworth, G. and Schechter, P. L. 1983, ApJ, 266, 41
- Davies, R. L. and Birkinshaw, M. 1988, ApJS, 68, 409
- de Vaucouleurs, G. et al. 1991, Third Reference Catalogue of Bright Galaxies, Springer-Verlag Berlin Heidelberg New York
- di Nella, H., Garcia, A. M., Garnier, R. and Paturel, G. 1995, A&A, 113, 151

- Dressler, A. 1984, ApJ, 286, 97
- Dwek, E. A. et al. 1995, ApJ, 445, 716
- Efron, B. and Tibshirani, R.J. 1993, An introduction to the bootstrap, Chapman & Hall, New York
- Ferrarese, L., van den Bosch, F. C., Ford, H. C., Jaffe, W. and O'Connell, R. W. 1994, AJ, 108, 1598
- Ferrarese, L., Ford, H.C. and Jaffe, W. 1996, ApJ, 470, 444
- Ferrarese, L. and Ford, H.C. 1999, ApJ, 515, 583
- Ferrarese, L. and Merritt, D. 2000, ApJ, 539, L9
- Ford, H.C. et al. 1994, ApJ, 435, L27
- Franx, M., Illingworth and G., Heckman, T. 1989, AJ, 98, 538
- Fried, J. W. and Illingworth, G. D. 1994, AJ, 107, 992
- Gebhardt, K. et al. 2000a, ApJ, 539, L13
- Gebhardt, K. et al. 2000b, AJ, 119, 1157
- Gebhardt, K. et al. 2003, ApJ, 583, 92
- Graham, A.W., Erwin, P., Caon, N. and Trujillo, I. 2001, ApJ, 563, L11
- Greenhill, L.J. and Gwinn, C.R. 1997, Ap&SS, 248, 261
- Heckman, T. M., Illingworth, G. D., Miley, G. K. and van Breugel, W. J. M. 1985, ApJ, 299, 41
- Kochanek, C. S. 1994, ApJ, 436, 56
- Kormendy, J. 1988, ApJ, 335, 40
- Kormendy, J. et al. 1996, ApJ, 459, L57
- Lauer, T. R 1985, ApJS, 57, 473
- Lauer, T. R. et al. 1992, AJ, 103, 703
- Launhardt, R., Zykla, R. and Mezger, P. G. 2002, A&A, 384, 112
- Maciejewski, W. and Binney, J. 2001, MNRAS, 323, 831
- Magorrian, J. et al. 1998, AJ, 115, 2285
- Marconi, A. and Hunt, L. 2003, ApJ, 589, 21

- Merritt, D. and Ferrarese, L. 2001, MNRAS, 320, L30
- Peletier, R. F., Davies, R. L., Illingworth, G. D., Davis, L. E. and Cawson, M. 1990, AJ, 100, 1091
- Peletier, R. F. et al. 1999, ApJS, 125, 363
- Press, W. H. et al. 1992, Numerical Recipes in C, Cambridge University Press, 2nd edition
- Sánchez-Portal, M., Díaz, Á. I., Terlevich, R., Terlevich, E., Álvarez Álvarez, M. and Artxaga, I. 2000, MNRAS, 312, 2
- Schödel, R. et al. 2002, Nature, 419, 694
- Tonry, J. L. et al. 2001, ApJ, 546, 681
- Tremaine, S. 1995, AJ, 110, 628
- Tremaine, S. et al. 2002, ApJ, 574, 740
- van den Bosch, F. C. and van der Marel, R. P. 1995, MNRAS, 274, 884
- van der Marel, R. P. 1994 MNRAS, 270, 271
- van der Marel, R. P. and van den Bosch, F. C. 1998, AJ, 116, 2220
- Verolme, E. K. et al. 2002, MNRAS, 335, 517